

Improved Titanium Machining: Modeling and Analysis of 5-Axis Toolpaths via Physics-Based Methods

Troy MARUSICH¹, Shuji USUI¹, Luis ZAMORANO¹, Kerry MARUSICH¹, Yoshihiro OOHNISHI²

¹Third Wave Systems, Inc., USA, sales@thirdwavesys.com

²ITOCHU Techno-Solutions Corporation, Japan, yoshihiro.oonishi@ctc-g.co.jp

Abstract:

Manufacturing monolithic components entails development of complicated five-axis toolpaths containing thousands of lines of code and dozens of tool changes for milling and drilling operations. Achieving meaningful reduction of cycle time while maintaining part quality is predicated upon the ability to model the physics of machining operations. A methodology to predict forces used for analyzing large, complicated five-axis toolpaths is presented. Forces and temperatures are predicted over the entire toolpath using analytical and numerical techniques to extend an empirical database to generalized cutting conditions. A method to achieve tangible reduction in cycle time without affecting part quality is presented.

Keywords: CAD/CAM systems, Process improvement, Simulation, Software, Optimization, Titanium

1. Introduction

Five-axis toolpaths can result in thousands of cutter orientations with respect to the workpiece, and are often used in the machining of complex monolithic aerospace components. Apart from tool orientations and multiple tool call outs, defining accurate cutter geometries, including the rake angles, corner radii, helix angles, etc.; calculating surface-surface intersections between workpiece and tool geometries as a function of feeds and speeds; defining workpiece geometries (of the order of several meters) while resolving chip loads (of the order of a few micrometers); all of these are computationally expensive procedures.

In addition to complicated toolpaths, the machining of titanium alloys and other high temperature aerospace metals pose additional challenges due to low thermal conductivity, high specific cutting power [[1]] and high hardness.

Commercially available verification software products provide methods to optimize the toolpaths but do not incorporate material behavior or cutting force prediction [[2]-[3]]. Several empirical models to predict cutting forces in machining processes have been well documented in literature [[4]-[8]]; yet, these models are not sufficient to simulate the machining of complex aerospace components utilizing five-axis toolpaths and predict forces for thousands of cutter locations and dozens of tools in a quick and efficient manner.

However complicated, implementing toolpath analysis into process design can yield a wide range of benefits in many different areas. With the help of a validated five-axis toolpath analysis model that can predict forces at each cutter location, cycle times and scrap can be reduced, and machine breakdown can be avoided, all through off-line analysis. Productivity and process efficiency can be improved through simulation, drastically reducing testing setup and cut time.

2. CAD Geometry and Toolpath Import

Prediction of cutting forces requires identification of chip thickness and local cutting edge geometry along the flutes or contour of the cutting tool. Machining houses that manufacture monolithic aerospace components use complicated five-axis toolpaths typically generated with CAM packages [[9]-[10]]. Commercially available verification software [[2], [11]] can simulate the workpiece and tool geometries in either their own proprietary formats or in more universally accepted formats such as STP and STL files. While these packages provide a capability to import CNC toolpaths in generally accepted formats (such as G-code or APT code) and import the tool and workpiece geometry, none of these packages consolidate geometric information such as chip thickness and chip shape with material behavior of high temperature alloys to give a unified predictive model which considers the geometry as well as material behavior. The force model presented in this paper utilizes its own solid modeling technology which allows capturing of the chip loads and process parameters such as cutting speeds, radial and axial depths of cut, etc.; the data from which is in turn fed into the force calculation kernel described in the next section.

The output of this model is thus in terms of forces, torque and horsepower rather than just chip load and other process parameters such as cutting speeds.

A variety of helical end mill geometries are used in the metal cutting industry. Helical cylindrical, ball end, taper helical ball, ball nosed and special purpose end mills are widely used in aerospace, automotive and die machining industries. Similar varieties also exist in drilling geometries. While the geometry of each cutter may be different, the mechanics of the milling process at each cutting edge point are common. The model presented in this paper discretizes the cutting geometry and applies empirically generated force data based on material behavior.

3. Semi-Empirical Modeling

3.1 Force Predictions

Correlating the discretized force computations to the five-axis toolpath geometry is the most critical aspect of modeling the physics of machining operations. The methodology presented herein utilizes a semi-empirical approach to capture the material properties in the form of force data. The force data is generated experimentally as a function of several variables such as cutting speed, feed, and tool geometry (back rake, side rake angles, etc.). Typically, force data is captured by performing tube turning measurements since these represent the simplest approach to capturing oblique cutting data. The data is captured in the form of axial, radial and tangential forces.

Thus for each material, tests are performed for several cutting conditions to cover the typical range of speeds, feeds and tool geometries in terms of rake angles [[12]].

3.2 Experimental Validation

The model presented in this paper includes a material database that contains multiple materials, including commonly used aerospace and automotive materials such as titanium, nickel, aluminum and steel alloys. Many standard tool geometries are also either readily available or can be imported in STP or STL format. This section contains a comparison between measured and predicted forces for validation from several different sources.

The first case is a validation of the force model in predicting drilling forces. Commonly used aerospace material Ti-6Al-4V was used as the workpiece material for modeling and testing. Forces were recorded using a Kistler 9255B table mounted dynamometer at Third Wave Systems' Productivity Center in Minneapolis, Minnesota. A total of 8 cases were machined to measure both tangential (F_t) and normal (F_n) forces against predicted data. Figure 1 shows the comparison of measured and predicted force values.

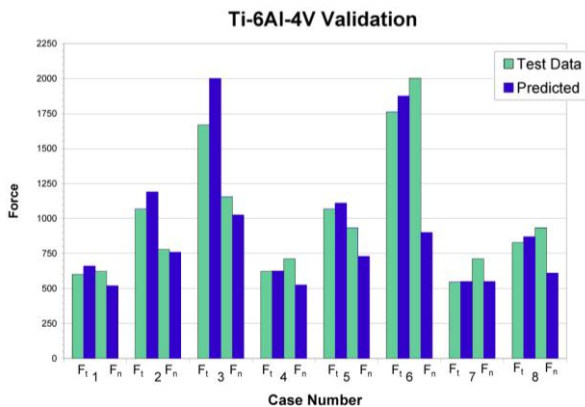


Figure 1: Force comparison predicted by AdvantEdge FEM and measured by dynamometer.

A second case is a validation of the force model predicting milling forces, as well as the material model prediction for chip shape. Figure 2 shows a machined

chip, as well as the predicted chip behavior as modeled in AdvantEdge FEM 3D.

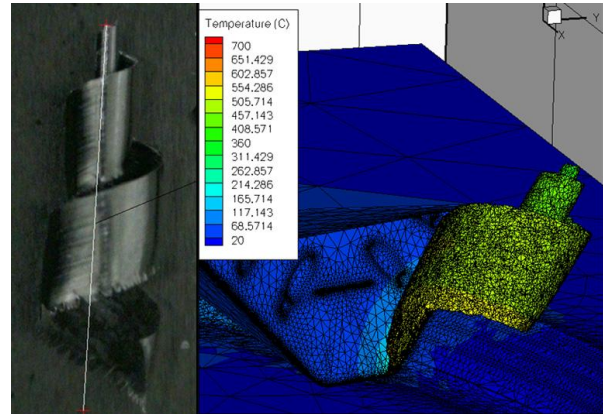


Figure 2: Experimental test chip and predicted chip shape as modeled in AdvantEdge FEM 3D.

Figure 3 shows the predicted and measured forces of the milling operation along the X-, Y-, and Z-axes. This case was run at a speed of 146 RPM with a feed per tooth of 0.1 mm and a 40% radial depth of cut.

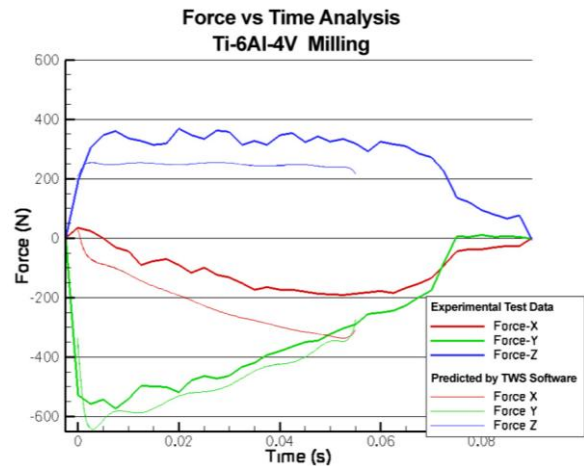


Figure 3: Milling force comparison predicted by AdvantEdge FEM and measured by dynamometer.

The third case is a validation of a force model predicting power exerted on a Ti-6Al-2Sn-4Zr-2Mo workpiece. Figure 4 shows the measured spindle power labeled "TMAC" compared with predictions of the force model labeled "PM" for the semifinishing pass. Spindle power was measured using Caron Engineering Tool Monitoring Adaptive Control-TMAC system [13]. The experimentally measured power consumption was then compared with the prediction of force model. Instantaneous deviations between predicted and measured spindle powers measurements can be primarily explained as the dynamic effects of the machine tool system that are captured experimentally.

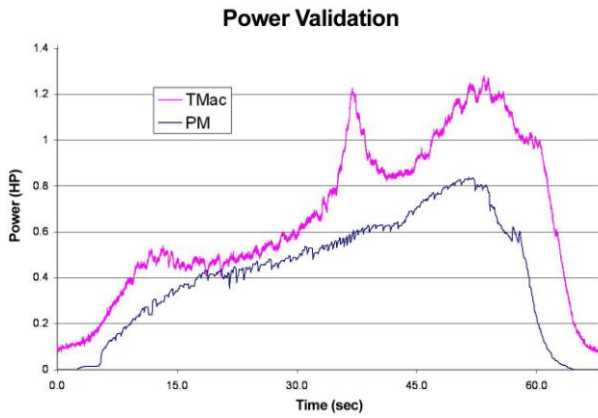


Figure 4: Semifinishing spindle power comparison predicted by model and measured by TMac.

4.0 Load Balancing

With a validated model that predicts cutting forces (tool coordinate system: tangential, axial and radial; or workpiece coordinate system: X, Y and Z), torques, and spindle power, the next logical step is to utilize this model to identify areas of improvement to reduce cycle times without affecting the productivity.

Productivity improvements can be achieved by increasing the feeds or speeds during the cut. To increase the rate at which the tool is fed while performing a five-axis machining operation on a high temperature alloy such as a titanium or nickel alloy, material behavior and specific cutting power should be considered in addition to the tool-workpiece interactions from a purely geometric perspective. This is achieved by using the force model generated using the techniques illustrated in the “Semi-empirical” modeling section of this paper.

To increase productivity, we used an approach called “load balancing,” analyzing cutting forces on the tool (e.g. tangential force) along the entire toolpath. There are instances where forces are at their peak, while at other instances along the toolpath, the same tool encounters much lower cutting forces. This is primarily an outcome of tool-workpiece geometric interaction (feeds, tool orientation, tool, and workpiece geometry) and workpiece material behavior (edge and corner radius effects on the chip load and cutting forces). We analyzed the entire toolpath and computed the cutting forces encountered by the tool as well as the workpiece during the entire toolpath for each cutter location, for all the tools being called out.

Consider a typical multi axis pocketing operation as shown in Figure 5. The tool enters the pocket at the bottom center and gradually cuts the pocket from “inside-out” rectangular motion. In some CAM packages this is referred to as “outward helical” operation.

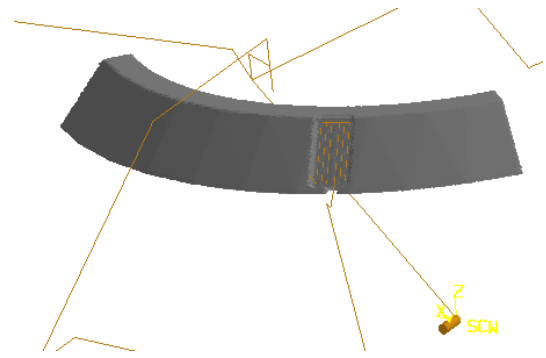


Figure 5: Multi-axis pocketing feature.

The tangential force signature pocketing encountered by the tool during this pocketing operation with the workpiece material Ti-6Al-2Sn-4Zr-2Mo is shown in Figure 6.

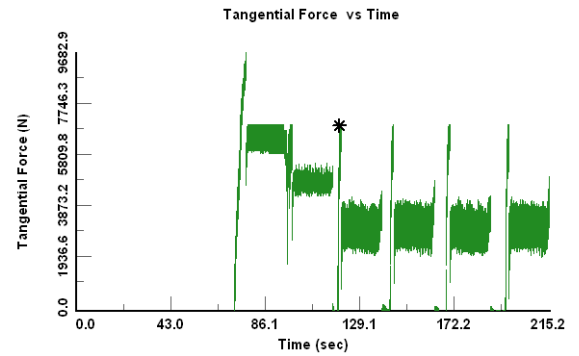


Figure 6: Tangential force encountered by tool.

Notice that the maximum forces are encountered at the beginning of the pocketing operation when the tool plunged blindly into the workpiece. While cutting speeds and feeds were kept constant throughout the pocketing operation, the chip load encountered by the tool varied throughout the pocketing operation. The tool initially encountered a peak force of 9682 N; for subsequent passes, it encountered forces of the order of 6964 N. Thus it was possible to increase the feeds in this sequence where the peak tangential forces encountered by the tool were still less than the total peak tangential force encountered by this tool during the entire operation.

The results as shown in Figure 6 above are considered to be the baseline for load balancing. The load balancing approach essentially analyzes each line of toolpath (G-code, APT code, etc.) and calculates the cutting forces (eg. tangential force). At each cutter location the model then compares these calculated cutting forces against the upper and lower force limits set by the user. If the allowable force is higher than the currently calculated force, the feed is increased to achieve the maximum allowable force. If the allowable force is lower than the force calculated in the baseline, the feed is reduced proportionately to achieve a lowered force. In this sense, the word optimization is used to indicate the load balancing approach; these two phrases are used interchangeably throughout the rest of this paper.

For the baseline force signature shown in Figure 6, if we specify a minimum force limit of 7100 N and keep

the maximum force limit of 9682 N, the optimization yields a new sequence time of 119.8 seconds. With a baseline sequence time of 215.2 seconds, this means an approximate savings of 44% as shown in Figure 7. Notice that the peak force encountered by the tool did not exceed the original maximum value of 9682 N.

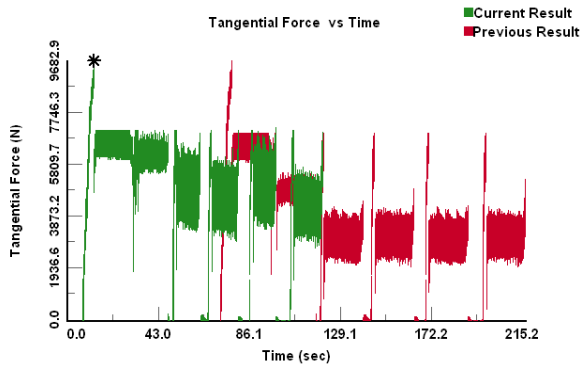


Figure 7: Comparison of baseline (previous result) and optimized (current result) force signatures.

It is important to note that during the load balancing approach, spindle speeds were kept unchanged. To better explain the selective feed changes, consider the example illustrated in Figure 8. This figure shows the “baseline” tangential forces encountered by a tool while cutting a jet engine component of Inconel-718. Notice that peak forces encountered by the tool were of the order of 350 N, where as there were several places where the tool encountered a force of 70 N. Thus by selectively increasing the feeds in these regions, it was possible to increase productivity without exceeding the maximum forces encountered by the tool. Figure 9 shows the force profile after optimization. Thus total cycle time of 837 seconds per pocket was reduced to a new cycle time of 723 seconds.

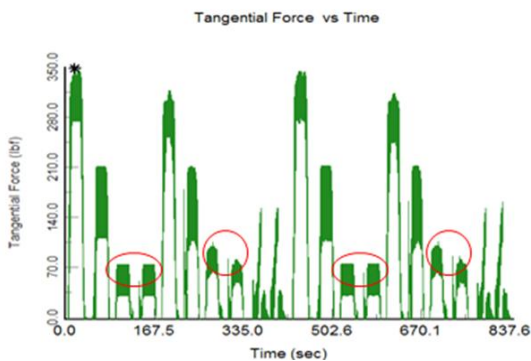


Figure 8: Baseline force signature for pocketing operation.

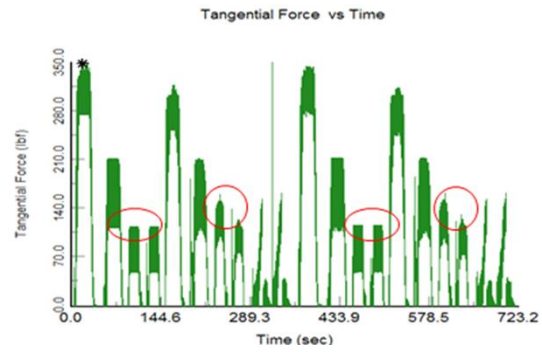


Figure 9: Optimized force signature for pocketing operation.

The feed profile of this pocketing operation before optimization is shown in Figure 10. Notice that after load balancing, feeds in only selective places are changed as shown in Figure 11.

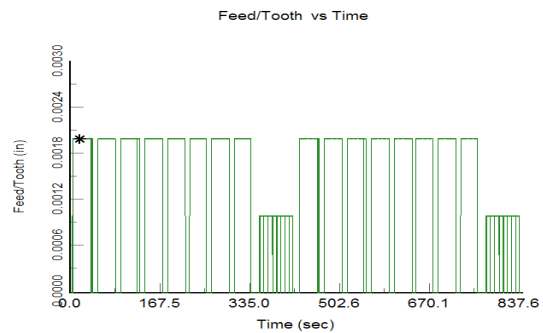


Figure 10: Feed profile for the pocketing operation.

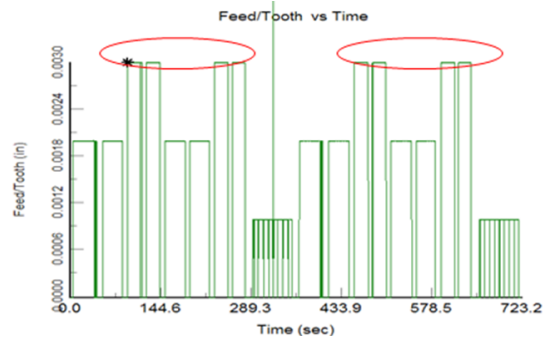


Figure 11: Selective feeds changed to increase productivity.

5.0 Application to Aerospace Components

Consider an aerospace part machined from a Ti-6Al-4V rectangular plate with dimensions of 900 mm x 150 mm x 25 mm. The minimum thickness of the walls was 2 mm and the lowest feed/tooth was 0.076 mm/tooth. Thus this simulation represented a scale difference of 900 mm/0.076 mm – 11840X – to represent its longest to shortest length scales and capture several magnitude length scales in between.

Figure 12 shows the finished workpiece geometry along with the toolpath. This part called in three different tools to perform several pocketing operations on the rectangular plate to achieve the final part geometry. For the sake of the current example, only representative operations by each tool were considered;

thus, the total cycle time of the entire part was only a fraction of total cycle time of the real part. Each tool encountered different maximum and minimum chip loads and correspondingly different maximum and minimum cutting forces.

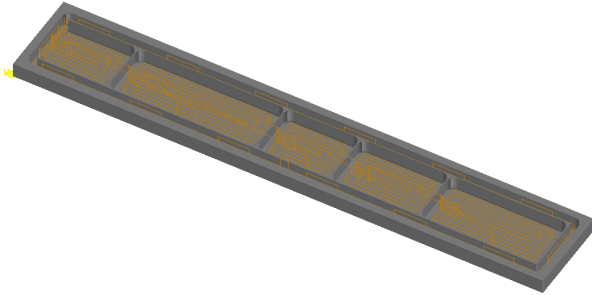


Figure 12: Aerospace pocket component.

Figure 13 shows the baseline results noted as “previous results” (tangential forces before load balancing) as well as optimized results noted as “current results” (tangential forces after load balancing.) The total machining cycle time for all three tools was reduced from 2355 seconds to 1644 seconds, approximately a 30% improvement in productivity.

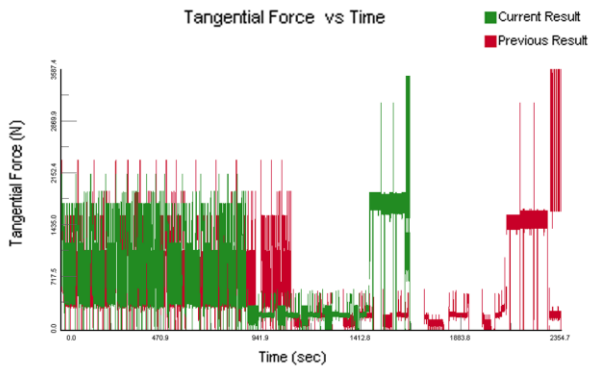


Figure 13: Comparison of baseline and optimized force signature.

It is important to note that the peak forces encountered by each tool were different and correspondingly, the limits of tangential forces used to balance the loads on each tool were set separately. For example, Tool 1 performed the pocketing operation shown in Figure 14. The peak tangential forces encountered during the baseline operation were of the order of 2610 N. These forces represent extreme loads that the tool encountered in pockets and corners.

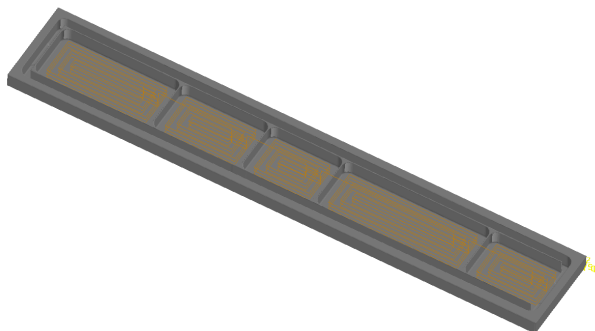


Figure 14: First pocketing operation.

While balancing the loads, it was theoretically possible to give a maximum force value of 2610 N and a minimum force value of 1750 N. But to avoid tool damage or poor tool life, it was recommended to use a maximum value of 2150 N. This is reflected in the “current results” where all the force values are peaking at or below 2150 N, as shown in Figure 15.

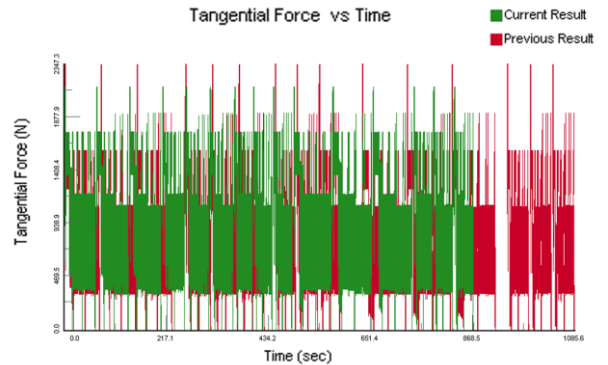


Figure 15: Optimized force signature for first pocketing operation.

The example above utilized only changes to the cutting feeds. Other approaches to further improve productivity, such as additional analysis using different tool geometries or toolpaths, are beyond the scope of this paper, yet yield even higher savings in cycle times using the same predictive force model presented here.

The next example is that of an engine rotor with workpiece material Ti-6Al-2Sn-4Zr-2Mo. In this example, apart from load balancing approach, changes to the tool geometry were also considered. The effect of changing tool geometry parameters such as the diameter along with cutting feeds was evaluated using the force model presented in this paper. The simulation setup required NC code, solid models, material properties, and tool geometry provided by the machining house that produces this component.

Figure 16 shows the simulation of rotor blade machining; the actual part machined is also shown for reference. The toolpath analysis approach involved splitting up the complete toolpath into separate features. The load balancing approach was used with automatic toolpath optimization capability presented earlier.

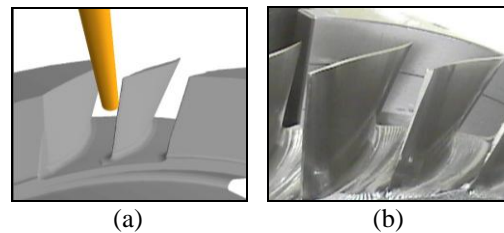


Figure 16: Simulation of (a) rotor blade machining and (b) actual rotor blades.

Each blade involved six different operations at various levels of feeds and speeds that cover a range of roughing to finishing operations. Figure 18 shows the baseline and optimized cycle-times for all six operations. For example, the toolpath for Operation 2 consisted of

two five-axis peripheral milling passes with a right- and left-hand flute tool. Using optimization bounds of 750 N to 1000 N for tangential force, the cycle time of one of the milling passes was reduced from 1.9 minutes to 1.2 minutes, or 37%. Figure 17 shows the plot of tangential force versus machining time. The original (baseline) toolpath is light grey and the optimized toolpath is dark grey. Load balancing of this toolpath shows that while the peak force was not increased, machining time was significantly decreased by adjusting feed rates.

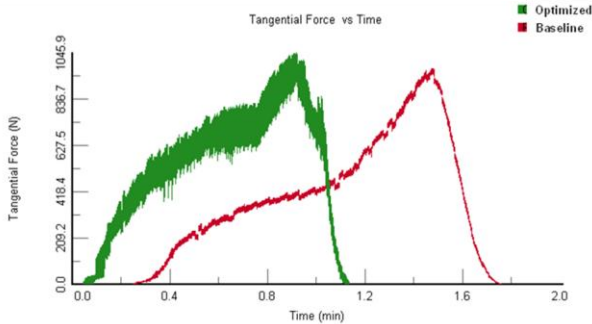


Figure 17: Force signature of Operation 1.

It is important to note that the force model presented in this paper is not necessarily used only for load balancing. Op1 presented in Figure 18 shows no distinguishable cycle time savings after performing analysis; however, a change in and analysis of the tool geometry in Op1 resulted in increased material removal while maintaining the same cycle time. Consequentially, this resulted in increased confidence in performing load balancing in Op2 since the chip loads and the cutting forces for Op2 were lowered.

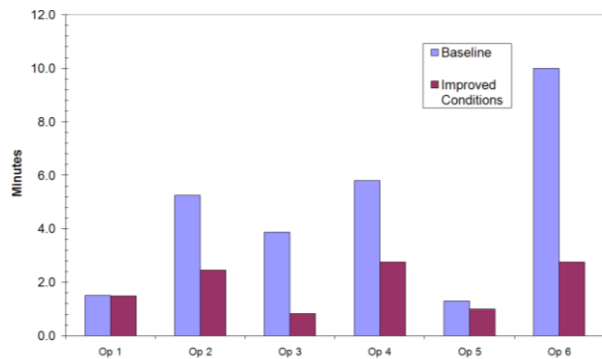


Figure 18: Six operations involved in engine rotor component.

6.0 Conclusion

An accurate prediction of five-axis machining process behavior, including cutting forces and horsepower consumption, is necessary for the understanding of the process and subsequent improvements to be made. It is possible to predict forces over the entire toolpath using analytical and numerical techniques to extend an empirical database to generalized cutting conditions. This semi-empirical model is able to predict torque and cutting forces encountered by the tool for drilling and milling operations. Using the same model, it is also possible to achieve a tangible reduction of cycle time while maintaining part quality.

References

- [1] Stephenson, D.A., Agapiou, J.S., 2006, Metal Cutting Theory and Practice, Second Edition, CRC, Boca Raton, FL, 19.
- [2] CG Tech, Vericut, www.cgtech.com/usa/products.
- [3] Diehl, S.A., "TrueMill® White Paper," www.surfware.com/truemill_toolpath_strategies.aspx
- [4] DeVor, R. E.; Kline, W. A., Zdeblick, W. J., A Mechanistic Model for the Force System in End Milling with Application to Machining Airframe Structures, 1980, Proceedings of the 8th North American Manufacturing Research, 297.
- [5] Nakayama, K., Arai M., Takei K., 1983, Semi-empirical equations for three components of resultant cutting force, Annals of the CIRP, 32/1: 33-35.
- [6] Brown, C.A., 1983, A Practical Method for Estimating Forces from Tool-chip Contact Area, Annals of the CIRP, 32/1: 91-95.
- [7] Stephenson, D.A., Agapiou, J.S., 1992, Calculation of Main Cutting Edge Forces and Torque for Drills with Arbitrary Point Geometries, International Journal of Machine Tool Manufacturing, 32/4: 521-538.
- [8] Srinivas, B.K., 1982, The Forces in Turning, SME Technical Paper, MR82-947.
- [9] Siemens PLM Software, NX CAM, www.plm.automation.siemens.com/en_us/products/nx/machining/machining/index.shtml.
- [10] Dassault Systems, CATIA www.3ds.com/products/catia/catia-discovery.
- [11] Predator Software Inc., Predator SDK, www.predator-software.com/virtualcnc.htm.
- [12] Stephenson, D.A., Bandopadhyay, P., 1997, Process-Independent Force Characterization for Metal Cutting Simulation, Transactions of the ASME Vol. 119.
- [13] Caron Engineering, Inc., www.caron-eng.com.